FINITE-DIFFERENCE REVERSE-TIME MIGRATION BASED ON ANISOTROPIC PURE QP WAVE EQUATION IN TTI MEDIA.

YUJIAN ZHANG JIANPING HUANG QIANG MAO

[a]School of Computer and Information Technology, Northeast Petroleum University, Da Qing, Heilongjiang, 163318, China;
Corresponding author: ZHANG Yan

ABSTRACT

The anisotropic effects in real earth media can induce waveform distortion on seismic wave propagation. Neglecting these effects in seismic imaging processing can lead to a degradation in imaging resolution. Therefore, starting from the exact P-wave dispersion relation, we derive a pure acoustic wave equation for tilted transversely isotropic (TTI) media to accurately characterize the anisotropic effects. In contrast to the coupled pseudo-acoustic TTI wave equation, our new pure acoustic TTI wave equation generates a noise-free wavefields and remains stable for anisotropic parameters ($\varepsilon < \delta$). The newly derived pure acoustic TTI wave equation accurately simulates the P-wave kinematic features, as demonstrated through theoretical analysis. Additionally, building on the proposed wave equation, we formulate a finite-difference operator and obtain a pure acoustic TTI wave equation that can be solved by finite-difference (FD) method. Numerical tests illustrate that the proposed FD-solvable pure acoustic TTI wave equation is highly efficient in wavefield simulation. Finally, based on the newly derived FD-solvable pure acoustic TTI wave equation, we implement TTI reverse time migration (TTI RTM). Numerical examples demonstrate the efficacy of the proposed TTI RTM scheme in correcting for anisotropic effects.

INTRODUCTION

The anisotropy effects of the real earth media are widely existed in underground, as evidenced through rock experiments and physical measurements (Thomsen, 1986; Tsvankin, 1996; Alkhalifah, 1998). These effects induce waveform distortion in the propagation of seismic wave, inevitably resulting in degraded imaging quality if their effects are disregarded. To obtain high-quality imaging results in anisotropic media, it is necessary to consider the effects of anisotropy and migrate their effects efficiently in imaging process.

Although anisotropic full elastic wave equation can accurately describe the propagation of seismic wave in anisotropic medium, it is difficult to be applied in petroleum industry due to its high computational cost and complexity (Cheng and Fomel, 2014; Zhu, 2017). Therefore, most exploration methods utilize P-wave only and simplify the full elastic wave equation to anisotropic acoustic equation for wavefield modeling and reverse time migration (RTM) (Li and Zhu, 2018; Zhu et al.,2018). Following that, a lot of approximations and assumptions (e.g., small angle approximation, elliptical approximation, weak anisotropy approximation and acoustic approximation) have been introduced to obtain qP wave equations (Fletcher et al., 2009; Zhang et al., 2011; Mu et al., 2020) over the years. Acoustic approximation introduced by Alkhalifah (1998) plays a crucial role in the derivation of pure qP wave equations. According to acoustic approximation, which states that the S-wave velocity along the axis of symmetry is zero. In comparison to aforementioned methods, the merits of acoustic approximation are reasonable accuracy and low computational cost. Afterward, Alkhalifah (2000) derived a coupled pseudo-acoustic wave equation using the acoustic approximation. However, this equation involves fourth-order partial derivatives in time-space domain, resulting in a large amount of computational resources for numerical simulation. To address these issues, some scholars simplified the fourth-order equations into second-order partial derivations utilizing an auxiliary wavefield (Zhou et al., 2006a; Fletcher et al., 2009; Flower et al., 2010). The wavefields simulated by coupled pseudo-acoustic wave equations can accurately describe the kinematic accuracy of P-wave. However, the aforementioned coupled pseudo acoustic wave equations are unstable when anisotropy parameter ε < δ. Subsequently, several stable coupled pseudo-acoustic wave equations (Duveneck and Bark, 2011; Zhang et al., 2011) are derived for wavefield simulation. Nevertheless, wavefields simulated by these coupled pseudo-acoustic anisotropic equations still contain undesired S-wave artifacts, due to the acoustic approximation only guarantees the S-wave velocity to be zero along the symmetry axis and not in all directions (Grechka et al., 2004).

To overcome this shortcoming, researchers have proposed pure acoustic wave equations for simulating wavefields in anisotropic media. Chu et al. (2011), and Zhan et al. (2012) independently used the first-order Taylor-series expansion to approximate the phase velocity formula and derived the pure

acoustic wave equations with a similar expression. Compared to the coupled pseudo acoustic TTI wave equations, these pure acoustic TTI wave equations cannot accurately simulate kinematic behavior of P-wave. Subsequently, Chu et al. (2013) employed the high-order Taylor series expansion to achieve the high accuracy qP-wave simulation, while leads to the huge computational cost. Recently, some high-precision pure acoustic anisotropic wave equations have been developed for wavefield simulation. Schleicher and Costa (2016) derived the precise pure acoustic wave equations that are effective even for strongly anisotropic media. Li and Zhu (2018) and Mu et al. (2020a) independently derived the pure qP-wave equation with high accuracy in TTI media for wavefield simulation and RTM. In addition, by setting the S-wave to zero at all direction, Xu et al. (2020) proposed a new acoustic approximation and derived a pure qP-wave dispersion relation. In addition, based on the work of Xu et al. (2020), Mao et al. (2023) also developed an accurate pure qP-wave equation in attenuating tilted transversely isotropic media to characterize the attenuation and anisotropy of seismic waves. Li and Stovas (2021) introduced a decoupled approximation and derived a pure qP-wave equation in TTI media that can eliminate SV-energy completely. These pure acoustic TTI wave equations are critical for wavefield simulation, imaging and inversion in anisotropic media.

In recent decades, the numerical simulation of pure qP anisotropic wave equations has attracted great attention. Fomel et al. (2013) and Song et al. (2013) developed the low-rank approximation method to solve Alkhalifah's (2000) dispersion relation formula, successfully achieving the simulation of pure qP wavefields. The low-rank approximation, known for its convenience in solving mixed space-wavenumber operators, has found widespread application in seismic wave simulation (Cheng and Fomel, 2014; Cheng et al., 2016; Wu and Alkhalifah, 2014; Sun et al., 2016; Zhang et al., 2019). However, this method exhibits computational inefficiency in simulations involving complex media due to its limitation to model complexity. Zhan et al. (2013) introduced the finite-difference and pseudo-spectral method to solve the pure qP-wave equation. Recently, Xu and Zhou (2014) separated the original pseudo-differential operator into two numerical solvable operators: a differential operator and a scalar operator, then successfully realized finite-difference simulation of pure qP-waves (Liang et al., 2023). Additionally, the local spatial operators are used proposed to simulate seismic wave propagation in VTI and TTI media (Nikonenko and Charara, 2021, 2023). The pure acoustic TTI wave equation has significantly enhanced computational efficiency when simulated through finite-difference methods.

In this paper, starting from the exact pure P-wave phase velocity formula and inspired by the work of Xu and Zhou (2014), we derive a pure acoustic TTI wave equation that can be solved by the finite-difference (FD) method. Our new wave equation can accurately simulate the kinematic behavior of P-wave, as illustrated by the theoretical analysis. In addition, in comparison to the coupled pseudo acoustic TTI wave equation, the wavefields simulated

by the proposed FD solvable pure acoustic TTI wave equation free of S-wave artifacts and is stable when anisotropy parameter $\varepsilon < \delta$. Numerical tests show that the newly derived wave equation can produce highly efficient wavefields. Finally, we employ our new FD solvable pure acoustic TTI wave equation as forward engine to implement TTI RTM. Numerical examples demonstrate that the proposed TTI RTM can effectively correct for anisotropic effects and provide high-quality imaging profiles in anisotropic media.

This paper is organized as follows: First, we derive a new pure acoustic TTI wave equation that can be solved by the finite-difference method. The accuracy and computational efficiency of the newly derived wave equation is verified through several numerical tests. Subsequently, we apply the proposed wave equation to implement TTI RTM. Finally, numerical examples are used to demonstrate the effectiveness of the proposed TTI RTM.

THEORY

Derivation of the finite-difference solvable pure qP-wave equation

We start from the exact dispersion formula for vertical transverse isotropic (VTI) media (), expressed as

$$V_P^2(\phi) = \frac{1}{2}\left[v_{p0}^2\left(1 + 2\varepsilon\sin^2\phi\right) + v_{s0}^2 + X \right], \tag{1}$$

$$V_{sv}^2(\phi) = \frac{1}{2}\left[v_{p0}^2\left(1 + 2\varepsilon\sin^2\phi\right) + v_{s0}^2 - X \right], \tag{2}$$

$$\tag{3}$$

where ϕ denotes the phase angle, ε and δ are anisotropic parameters (Thomsen, 1986), respectively. According to equation (1), Alkhalifah (1998) set the v_{s0} to 0 (i.e., acoustic assumption) to reduce the number of required parameters, resulting in pure qP-wave dispersion relation. However, the coupled pure qP-wave equations derived from Alkhalifah's (1998) dispersion relation suffer from q-SV artifacts and are only applicable when $\varepsilon > \delta$. Therefore, it is necessary to develop stable and accurate pure qP-wave equations to address the above-mentioned issues.

Based on equation (2), we define a auxiliary function:

$$V_{sv}^2(\phi) = v_{p0}^2\left[2\varepsilon\sin^2\phi + 2\delta\sin^2\phi\cos^2\phi \right]. \tag{4}$$

By substituting this expression of $V_{sv}^2(\phi)$ into equation (2), v_{s0}^2 can be represented as follows:

$$v_{s0}^2 = V_{SV}^2(\phi) - 2(\varepsilon - \delta)\sin^2\phi\cos^2\phi \frac{v_{p0}^2 - V_{SV}^2(\phi)}{1 + 2\varepsilon\sin^4\phi + 2\delta\sin^2\phi\cos^2\phi - \frac{V_{SV}^2(\phi)}{v_{p0}^2}}, \tag{5}$$

According to expressions of $V_{sv}^2(\phi)$ and v_{s0}^2, the equation (1) can be approximated as

$$V_P^2(\phi) \approx v_{p0}^2\left(1+2\varepsilon\sin^2\phi\right)-2v_{p0}^2\left(\varepsilon-\delta\right)\sin^2\phi\cos^2\phi\frac{1-2\varepsilon\sin^2\phi-2\delta\sin^2\phi\cos^2\phi}{1-2\varepsilon\sin^2\phi\cos^2\phi}. \quad (6)$$

Because $2\varepsilon\sin^2\phi\cos^2\phi$ and $2\delta\sin^2\phi\cos^2\phi$ is small relative to 1, for most case. Many scholars neglect these terms, we set the trigonometric factor $\sin^2\phi$ and $\cos^2\phi$ to its average value of 0.5 instead of setting them to zero (Huang et al., 2023). As a result, equation (5) can be approximated as

$$V_P^2(\phi) \approx v_{p0}^2\left(1+2\varepsilon\sin^2\phi\right)-2v_{p0}^2\frac{(\varepsilon-\delta)}{1-0.5\varepsilon}\sin^2\phi\cos^2\phi\left[(1-0.5\delta)-2\varepsilon\sin^2\phi\right]. \quad (7)$$

Different from acoustic approximation, the above approximation avoids such coupled SV-wave artifacts. In addition, the relationship between wavenumber and phase angle can be given as

$$k_x = \omega\sin\phi/V_p(\phi), k_z = \omega\cos\phi/V_p(\phi). \quad (8)$$

Where k_x and k_z are the wavenumbers in the horizontal and vertical directions, and ω is angular frequency, respectively. Substituting eq. (7) into eq. (6), eq. (6) can be written as

$$\omega^2 = v_{p0}^2\left(1+2\varepsilon\right)k_x^2+v_{p0}^2k_z^2-\frac{2v_{p0}^2\eta}{\left(k_x^2+k_z^2\right)^2}\left[(\sigma-2\varepsilon)k_x^4k_z^2+\sigma k_x^2k_z^4\right], \quad (9)$$

$$\eta = \frac{(\varepsilon-\delta)}{1-0.5\varepsilon}, \quad (10)$$

$$\sigma = (1-0.5\delta). \quad (11)$$

The transformation relations between the time-space domain and frequency-wavenumber domain can be shown as follows:

$$i\omega \leftrightarrow \partial/\partial t, ik_x \leftrightarrow \partial/\partial x, ik_z \leftrightarrow \partial/\partial z. \quad (12)$$

Based on equation (12), multiplying both sides of equation (9) with the wavefields in wavenumber domain $p(\omega,k_x,k_y,k_z)$, we can obtain the time-space pure acoustic VTI wave equation as follows:

$$\frac{1}{v_{p0}^2}\frac{\partial^2 p}{\partial t^2} = (1+2\varepsilon)\frac{\partial^2 p}{\partial x^2}+\frac{\partial^2 p}{\partial z^2}-\frac{2\eta}{\left(\frac{\partial^2}{\partial x^2}+\frac{\partial^2}{\partial z^2}\right)^2}\left((1-0.5\delta-2\varepsilon)\frac{\partial^6 p}{\partial x^4\partial z^2}+(1-0.5\delta)\frac{\partial^6 p}{\partial x^4\partial z^2}\right)+s, \quad (13)$$

where s denotes the source function. Equation (13) can be conveniently simulated by pseudo-spectral (PS) method and hybrid finite-difference/pseudo-spectral (HFDPS) method. However, PS method and HFDPS method require uneconomic Fast Fourier transform (FFT) and inverse FFT, making

it computationally inefficient. To solve pure qP-wave equation efficiently, we derive a FD solvable pure qP-wave equation in the following derivation. According to Xu and Zhou (2014), we construct an operator as follows:

$$S_k = \frac{-2\eta k_x^2 k_z^2}{k_x^4 + 2k_x^2 k_z^2 + k_z^4}. \tag{14}$$

Substituting the operator S_k into equation (9), equation (9) becomes

$$\omega^2 = v_{p0}^2 \left((1+2\varepsilon) k_x^2 + k_z^2 \right) + v_{p0}^2 S_k \left((\sigma - 2\varepsilon) k_x^2 + \sigma k_z^2 \right). \tag{15}$$

By multiplying equation (16) with the wavefield $p(\omega, k_x, k_z)$ in the in the Fourier domain and transforming it into time-space domain, we can obtain the following pure qP-wave equation in VTI media:

$$\frac{\partial^2 p}{\partial t^2} = v_{p0}^2 \left((1+2\varepsilon) + (\sigma - 2\varepsilon) S_k \right) \frac{\partial^2 p}{\partial x^2} + v_{p0}^2 (1 + \sigma S_k) \frac{\partial^2 p}{\partial z^2}. \tag{16}$$

According to Zhan et al. (2012), the relationship between VTI and TTI media can be expressed as

$$\begin{bmatrix} \hat{k}_x \\ \hat{k}_z \end{bmatrix} = \begin{pmatrix} cos\theta & -sin\theta \\ sin\theta & cos\theta \end{pmatrix} \begin{bmatrix} k_x \\ k_z \end{bmatrix}, \tag{17}$$

$$\hat{k}_x^2 + \hat{k}_z^2 = k_x^2 + k_z^2, \tag{18}$$

where θ is the tilt angle. Substituting equations (17) and (18) into equation (15), the TTI dispersion relation can be expressed as

$$\omega^2 = v_{p0}^2 (1+2\varepsilon) \left(k_x^2 \cos^2\theta - 2k_x k_z \sin\theta \cos\theta + k_z^2 \sin^2\theta \right) + v_{p0}^2 \left(k_x^2 \sin^2\theta + 2k_x k_z \sin\theta \cos\theta + k_z^2 \cos^2\theta \right) + v_{p0}^2 S_k' \left((\sigma - 2\varepsilon) \left(k_x^2 \cos^2\theta - 2k_x k_z \sin\theta \cos\theta + k_z^2 \sin^2\theta \right) \right) + \sigma \left(k_x^2 \sin^2\theta + 2k_x k_z \sin\theta \cos\theta + k_z^2 \cos^2\theta \right) \right), \tag{19}$$

$$S_k' = \frac{-2\eta \left(k_x^2 \cos^2\theta - 2k_x k_z \sin\theta \cos\theta + k_z^2 \sin^2\theta \right) \left(k_x^2 \sin^2\theta + 2k_x k_z \sin\theta \cos\theta + k_z^2 \cos^2\theta \right)}{\left(k_x^2 + k_z^2 \right)^2}. \tag{20}$$

As per Liang (2023), The propagation direction is denoted as $\boldsymbol{n} = (n_x, n_z) = (sin\theta, cos\theta)$, which can represent the phase direction of wave propagation. The relation between k and θ is

$$\frac{k_x}{k} = sin\theta = n_x, \frac{k_z}{k} = cos\theta = n_z, \tag{21}$$

the unit vector $\boldsymbol{n}$ is rewritten as

$$\boldsymbol{n} = (n_x, n_z) = \left(\frac{k_x}{k}, \frac{k_z}{k} \right) = \frac{\boldsymbol{k}}{k} = \frac{\boldsymbol{k}}{|\boldsymbol{k}|}. \tag{22}$$

Substituting equation (23) into (14), equation (14) becomes

$$S_k = \frac{-2\eta\left(\frac{k_x}{k}\right)^2\left(\frac{k_z}{k}\right)^2}{\left(\left(\frac{k_x}{k}\right)^2+\left(\frac{k_z}{k}\right)^2\right)^2} \cdot = \frac{-2\eta n_x^2 \cdot n_z^2}{\left(\left(n_x\right)^2+\left(n_z\right)^2\right)^2}. \tag{23}$$

The asymptotic form of (23) in space is proposed by Xu et al (2014), that can be expressed as

$$\boldsymbol{n} = \nabla P / |\nabla P| = \left(\frac{\partial p}{\partial x}e_x + \frac{\partial p}{\partial z}e_z\right)\Big/\left\|\left(\frac{\partial p}{\partial x}e_x + \frac{\partial p}{\partial z}e_z\right)\right\|, \tag{24}$$

n_x and n_z are rewritten as

$$n_x = \frac{\dfrac{\partial p}{\partial x}}{\sqrt{\left(\dfrac{\partial p}{\partial x}\right)^2+\left(\dfrac{\partial p}{\partial z}\right)^2}}, n_z = \frac{\dfrac{\partial p}{\partial z}}{\sqrt{\left(\dfrac{\partial p}{\partial x}\right)^2+\left(\dfrac{\partial p}{\partial z}\right)^2}}. \tag{25}$$

Substituting equation (26) into (24), the operator can be expressed as

$$S_k \approx \frac{-2\eta\left(\dfrac{\partial p}{\partial x}\right)^2\left(\dfrac{\partial p}{\partial z}\right)^2}{\left(\left(\dfrac{\partial p}{\partial x}\right)^2+\left(\dfrac{\partial p}{\partial z}\right)^2\right)^2}. \tag{26}$$

Finally, the time-space domain pure acoustic TTI wave equation can be written as

$$\frac{1}{v_{p0}^2}\frac{\partial^2 p}{\partial t^2} = \left((1+2\varepsilon)\cos^2\theta+\sin^2\theta+\left((\sigma-2\varepsilon)\cos^2\theta+\sigma\sin^2\theta\right)S_k'\right)\frac{\partial^2 p}{\partial x^2}$$

$$\cdot -2\varepsilon\sin 2\theta\left(1-S_k'\right)\frac{\partial^2 p}{\partial x\partial z}+\left((1+2\varepsilon)\sin^2\theta+\cos^2\theta+S_k'\left((\sigma-2\varepsilon)\sin^2\theta+\sigma\cos^2\theta\right)\right)\frac{\partial^2 p}{\partial z^2}. \tag{27}$$

Accuracy analysis of the proposed wave equation (9)

Theoretical analysis is employed in this case to evaluate the accuracy of the proposed wave equation. The phase velocity curve comparisons between the exact phase velocity formula, the acoustic approximate formula, the proposed approximated formula, and Zhan et al.'s (2012) approximated formula are generated, as shown in Fig. 1. In order to evaluate the accuracy of the eq.9, we select four groups of typical parameters for accuracy analysis, as shown in Table 1.

Figure 1 describes the phase velocity curves of different formulas. The exact phase velocity formula is suitable for accessing the accuracy of the anisotropic acoustic equations. As shown in Figure 1, we can observe that our new wave equation is in better agreement with the exact phase velocity formula than that of Zhan et al.'s (2012) equation. This result indicates that the approximation we adopted is appropriate. In the following, we imply that the efficiency of the

proposed acoustic wave equation simulated by FD method is higher than the previous pure acoustic wave equations.

Table1. The parameters are used to generate the phase velocity curves.

Model type	v_{p_0}(m/s)	ε	δ
I	2500	0.3	0.1
II	2500	0.1	0.3
III	2500	0.4	0.05
IV	2500	0.1	-0.1
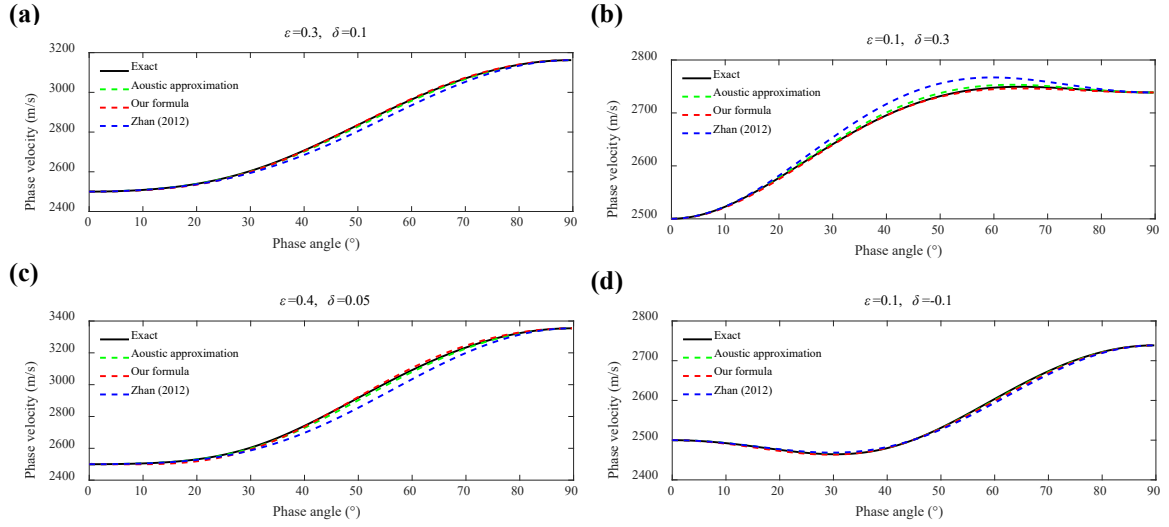
Figure 1. The phase velocity of P-wave using different anisotropy parameters. The black solid lines, blue dashed lines, red dashed lines, and green dashed lines denote the exact phase velocity formula of P-wave, Zhan et al.'s (2012) approximated formula, proposed approximated formula, and acoustic approximated formula, respectively. The model parameters from Fig. 1a-d are the sets of I-IV in Table 1.

Accuracy analysis of the proposed wave equation (21)

To verify the accuracy of our proposed FD-solvable wave equation in wavefield simulation, we designed a TTI homogeneous model. The computational domain is 601 × 601 with the grid spacing of 10m. A Ricker wavelet with the peak frequency of 25 Hz is used as source function, which located at (3005 m, 3005 m), and the time step is 0.001 s. Because the coupled pseudo-acoustic TTI wave equations are derived under pseudo-acoustic assumption can yield good kinematic approximation (Mu et al., 2020), we choose Duveneck et al.'s (2008) coupled pseudo-acoustic wave equation as reference for evaluating the accuracy of our equation. The PS method is used to solved the proposed wave equation in this part.

Figure 2 shows the wavefield snapshots at 1.0 s generated by Duveneck et al.'s (2008) coupled pseudo-acoustic TTI wave equation, Zhan et al.'s (2012) equation, and our newly proposed equation, respectively. In Figure 2, we can

observe that the wavefields simulated by the coupled pseudo-acoustic TTI wave equation produce the S-wave artifacts and become unstable when anisotropic parameters $\varepsilon < \delta$. However, the wavefields calculated by the proposed pure-acoustic TTI wave equation are noise-free and numerical stable.

Then, to verify the accuracy of the proposed wave equation, several traces extracted from Figure 2 at depth of 1010m and 4010m are plotted in Figure 3. As indicated in Figure 3, the proposed wave equation is in better match with the exact dispersion relation than that of Zhan et al.'s (2012) wave equation, which demonstrate the newly derived wave equation has higher accuracy than Zhan et al.'s (2012) pure acoustic wave equation.
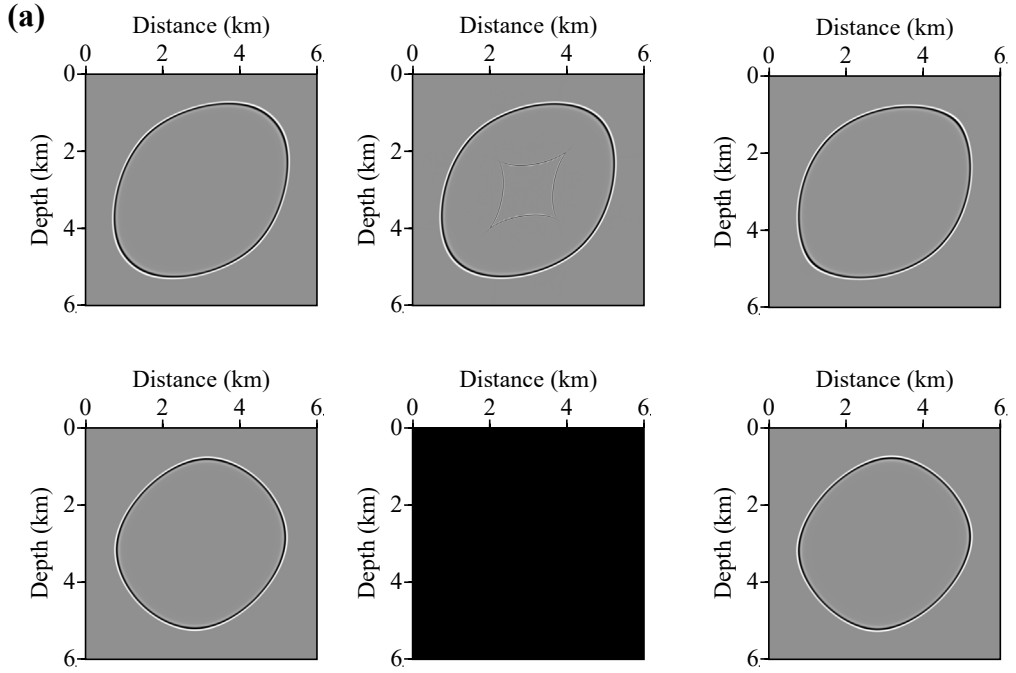
Figure 2 The snapshots of homogeneous model. (a) $\varepsilon = 0.35$, $\delta = 0.1$, $\theta = 45°$, (b) $\varepsilon = 0.1$, $\delta = 0.35$, $\theta = 45°$, (c) $\varepsilon = 0.35$, $\delta = 0.1$, $\theta = 45°$, (d) $\varepsilon = 0.1$, $\delta = 0.35$, $\theta = 45°$, (e) $\varepsilon = 0.35$, $\delta = 0.1$, $\theta = 45°$, (f) $\varepsilon = 0.1$, $\delta = 0.35$, $\theta = 45°$.
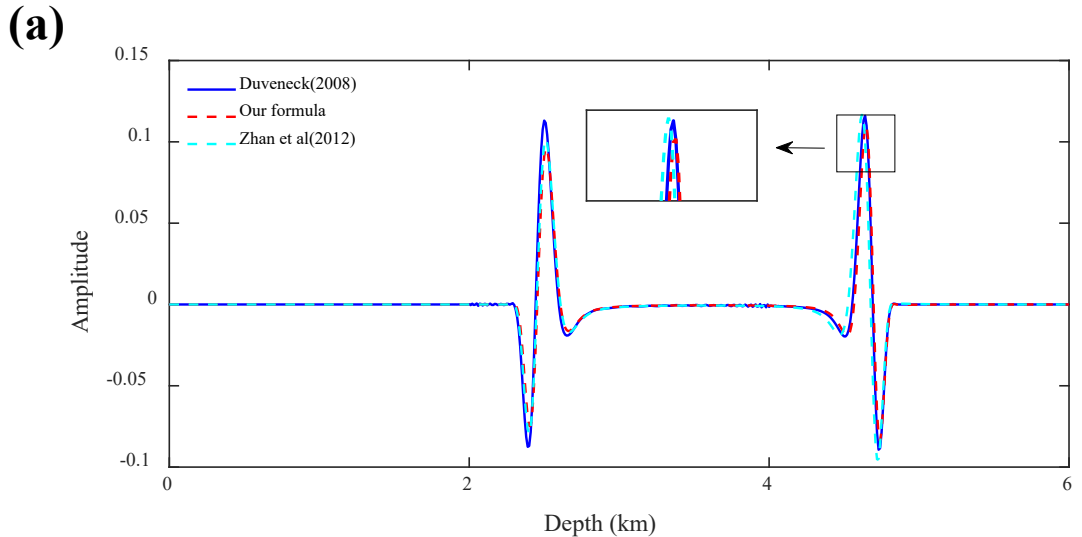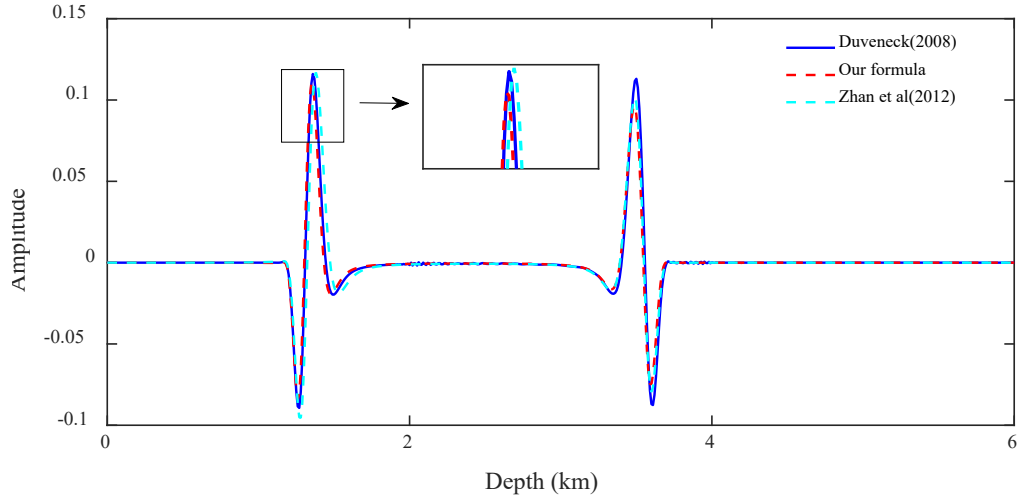
Figure 3. Comparison of traces at two vertical distances: (a) 1010 m, (b) 4010 m

Accuracy analysis of the proposed FD-solvable wave equation (27)

In this case, in order to validate the accuracy of the result solved by FD method, a homogenous TTI model is to illustrate the simulation accuracy of FD method for solving TTI pure acoustic equation (equation 27). The reference result is generated by the PS method.

The computational domain is 3010 m × 3010 m with a spatial step of 10m. A Ricker wavelet with the dominated frequency of 20 Hz is used as source function located at (1505 m, 1505 m), the time step is 0.001 s. The velocity of P-wave is 2500m/s, and we set the anisotropy parameters as $\varepsilon = 0.24$, $\delta = 0.18$ $\theta = 45°$. Figure 4 shows the wavefield snapshots simulated by the PS method and the FD method. Subsequently, two single-traces are extracted from Figure 4 at distance of x= 1.0 km and 2.5 km for clear comparison are depicted in Figure 5. As shown in Figure 5, this result demonstrates that the wavefield generated by the FD method can well preserve the phase (i.e., kinematics feature) of wavefield, and cannot remain the amplitude (i.e., dynamics feature) of the wavefield well. It is obvious that the two traces match each other well, which demonstrates that the accuracy of the proposed FD method is validated.
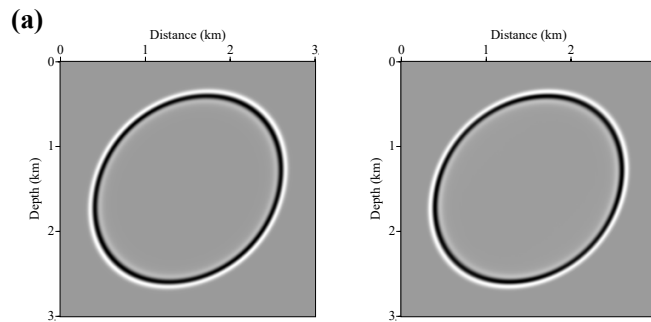

Figure 4 Snapshots of anisotropic model. (a) simulated by PS method ($\varepsilon = 0.24, \delta = 0.18, \theta = 45°$). (b) simulated by FD method ($\varepsilon = 0.24, \delta = 0.18, \theta = 45°$).
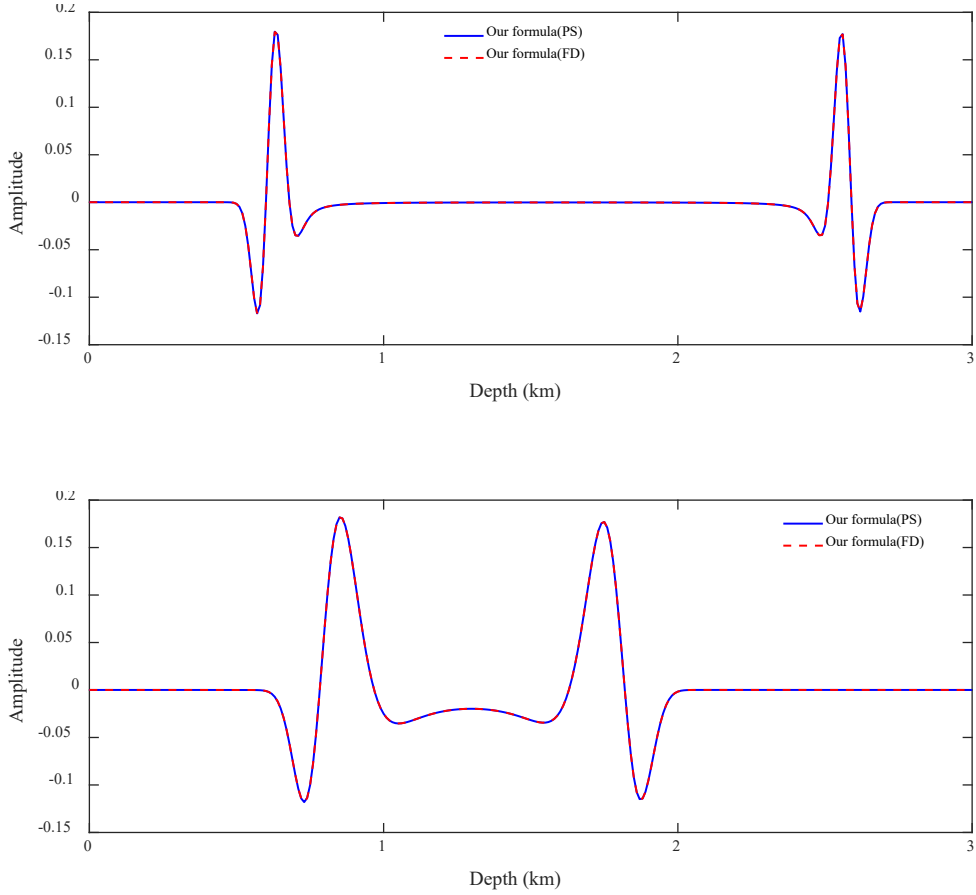
Figure 5 Comparison of traces at lateral distance: 1010 m and 2510m. The traces extracted from Figure 4a are represented by the solid blue line, the traces extracted from Figure 4b are represented by the dashed red line.

Computational efficiency analysis of the proposed FD-solvable wave equation

In this case, to illustrate the efficiency of the proposed FD-solvable equation, we provide the calculating time comparison between different propagation time under different simulation method, as shown in Table 2. The parameters are $v_p = 2500$ m/s, $\varepsilon = 0.3$, $\delta = 0.1$, $\theta = 45°$. A Ricker wavelet with the peak frequency of 25 Hz is used as source function.

Table 2 shows the calculation time of different propagation time under different simulation method. It is evident that the proposed equation simulated by FD method exhibits shorter calculation time than the other under the same propagation time. This result from Table 2 suggests that the proposed FD-solvable equation is more computationally efficient than the equation simulated by PS method. Based on this feature, our wave equation also has great application potential in 3D case due to its high computational efficiency. The numerical tests are performed on the Matlab software platform, utilizing a computer equipped with an Intel Core i5-10505@3.20 GHz processor, 8 GB of RAM, and a 1 TB/7200 rpm hard disk.

Table 2. Running time for simulating a wavefield for a homogeneous VTI model with different propagation times.

Homogeneous VTI model	Propagation time (s)	PS running time (s)	HFDPS running time (s)	FD running time (s)
Running time (s)	1s	943.357883	365.425422	84.378289
	2s	1985.280156	717.395381	175.149457
	3s	2941.558762	1069.563886	261.907284

Note that the compute platform is matlab software

NUMERICAL EXAMPLE

In this section, we perform RTM tasks in the Hess TTI model and Marmousi TTI model to demonstrate the feasibility and effectiveness of the anisotropic TTI RTM. We used the sponge boundary to absorb reflections.

Modified Hess TTI model

To further verify the feasibility of the proposed algorithm, we implement the anisotropic RTM in the Hess TTI model. The model parameters of Hess TTI model are shown as Figure 6a-d. The model size is 1206 ×500 with the grid size of 10m.We use a Ricker wavelet with the peak frequency of 25 Hz as source function. The 60 shots are evenly placed on the surface with a shot depth of 10 m. we use 1206 receivers to record the reflection data for each shot, the receiver depth is 10 m.

Figure 7 shows RTM imaging results based on the newly proposed pure acoustic equation. Figure 7a is used as reference, which is simulated by HFDPS method. And Figure 7b is solved by the proposed TTI RTM with FD method. In addition, there are no noise in shallow layer in Figure 7a and 7b. This test illustrates that TTI RTM can produce high-resolution imaging results.

Subsequently, in order to demonstrate the accuracy of the proposed RTM schemes using the FD method, we extract the single-traces comparison from Figure 7a and 7b, and shown in Figure 8. In Figure 8, we observe that the traces extracted from Figure 7b are in good agreement with that extracted from Figure 7a. This result demonstrates that the proposed RTM schemes using the FD solver can accurately image the structure.
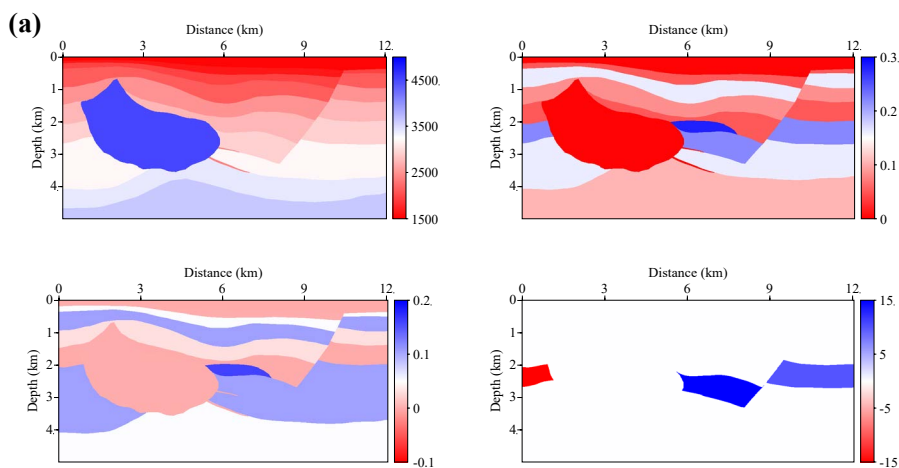
(a)

Figure 6 The anisotropy parameters of Hess TTI model. (a) v_p, (b) ε, (c) δ, (d) θ.
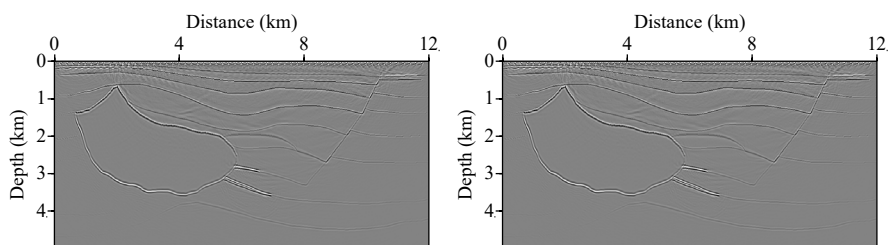

Figure 7. The reverse time migration of Hess TTI model. (a) TTI RTM (used as reference), (b) TTI RTM
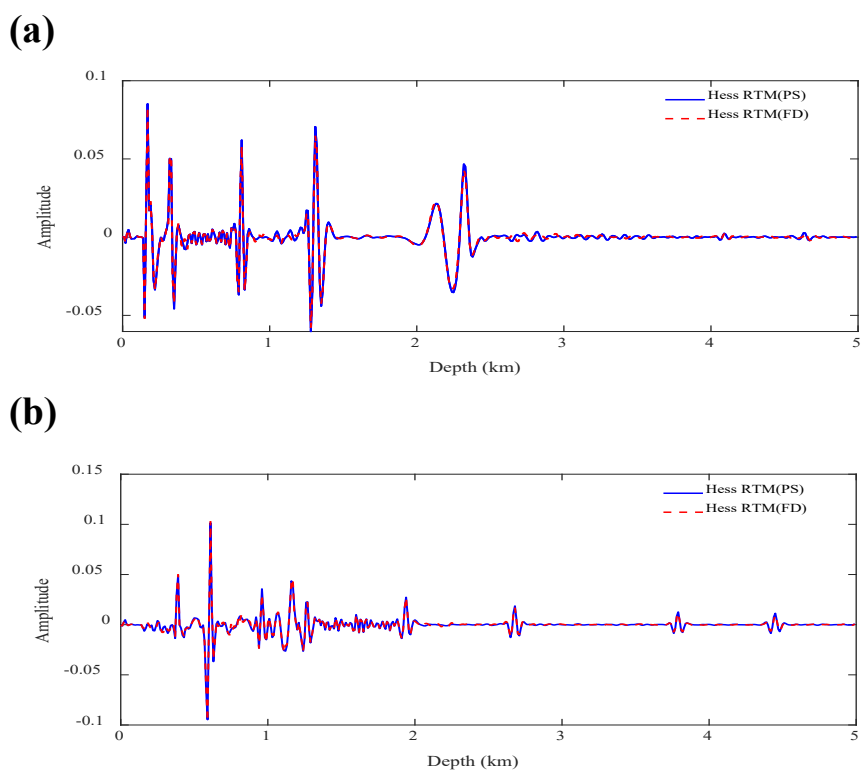
(a)

(b)

Figure 8. Comparison of traces at lateral distance: 1000 m and 10000m. The traces extracted from Figure 7a are represented by the solid blue line, the traces extracted from Figure 7b are represented by the dashed red line.

Marmousi TTI model

In this case, we choose Marmousi TTI model (Mu et al., 2020b) to further demonstrate the precision of the proposed TTI RTM scheme, the model parameters are shown in Figure 9a-d. This model is discretized into 369 × 188 grids with the grid interval of 12.5 m. A Ricker wavelet of the dominated frequency of 25 Hz is used as source function, and the time step is 0.0008 s. 60 shots are uniformly placed on the surface with the shot depth of 12.5 m. For each shot, we use 296 receivers to receive the shot record information, and receiver depth is 12.5 m.

Figure 10a-b show the imaging results computed by the newly proposed anisotropic acoustic equation. From Figure 10a-b, we can notice that the imaging results calculated by the pure acoustic TTI wave equation has the clear and continuous imaging interfaces. Then, in order to demonstrate the accuracy of the proposed TTI RTM based on the FD solver, we generate the single-traces comparison between the Figure 10a and Figure 10b, and shown in Figure 11. In Figure 11, we can observe that the traces extracted from the Figure 10b are in good consistence with that extracted from Figure 10a. This result suggests that TTI RTM performed by FD method is reliable. Furthermore, because the proposed TTI RTM based on the FD solver, which has high computational efficiency. Therefore, the proposed TTI RTM can be conveniently extended to 3D case to achieve high-resolution in anisotropic media.
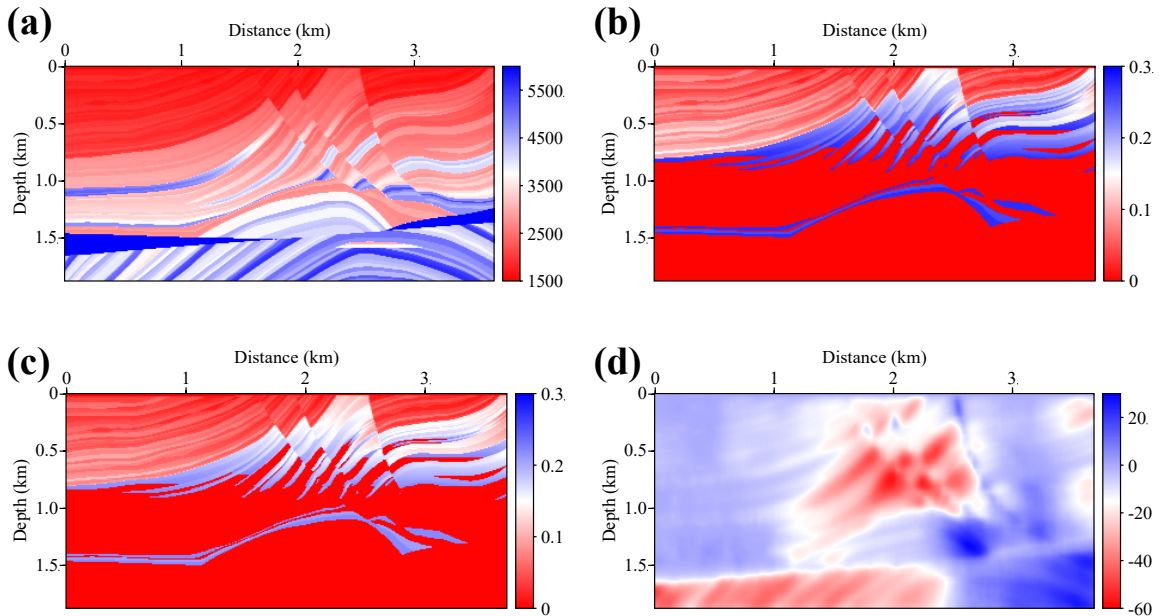
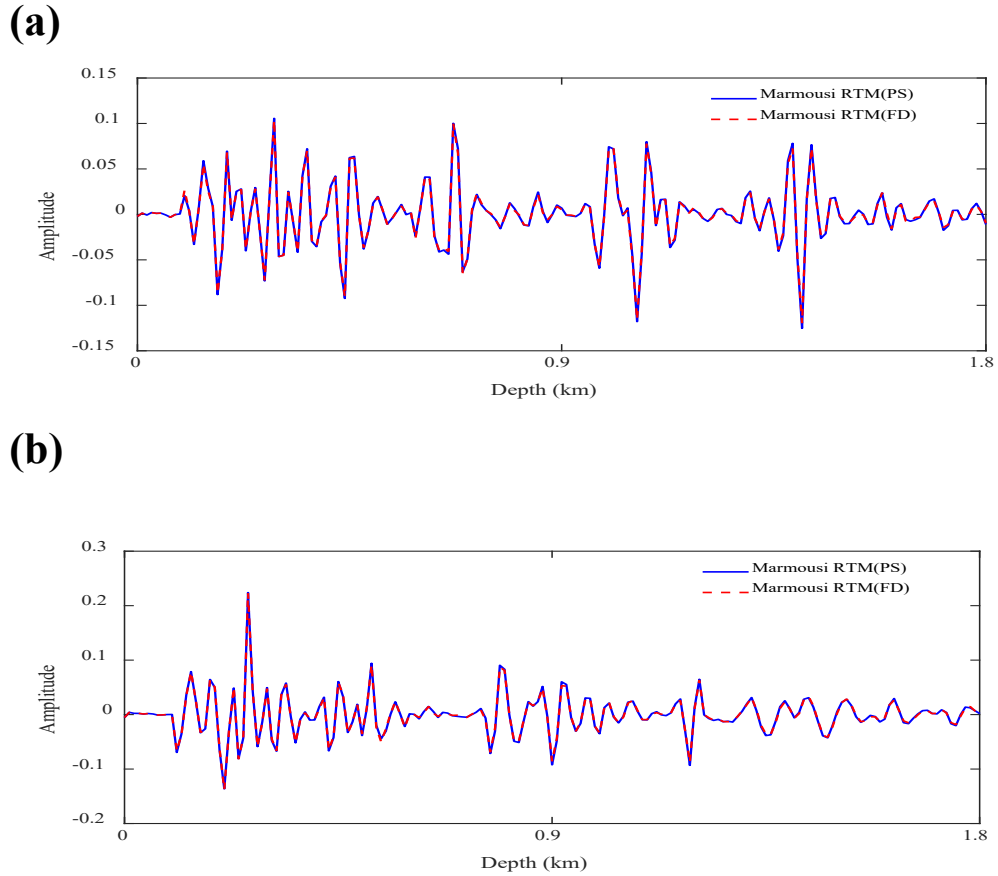Figure 9 The anisotropy parameters of Marmousi TTI model. (a) v_p, (b) ε, (c) δ, (d) θ.

(a)

(b)

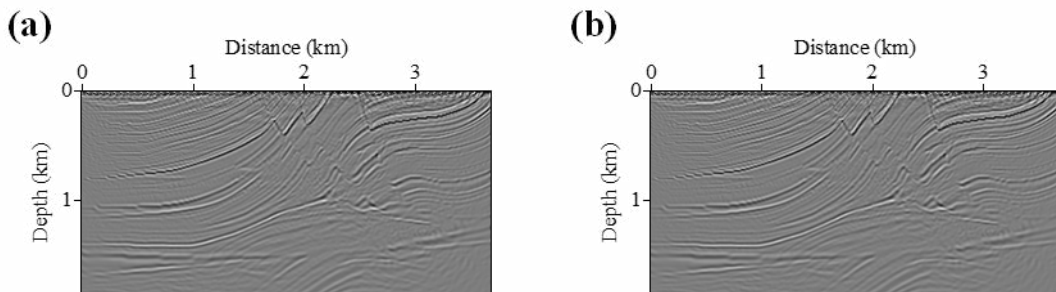Figure 10 The reverse time migration of Marmousi TTI model.

(a)

(b)

Figure 11 Comparison of traces at lateral distance: 1000 m and 3000m. The traces extracted from Figure 10a are represented by the solid blue line, the traces extracted from Figure 10b are represented by the dashed red line.

DISSCUSION

In this study, we derive a pure acoustic TTI wave equation with high precision. The FD method is introduced to efficiently solve our new wave equation. In this section, we discuss several crucial issues. Firstly, our new wave equation has high accuracy than Zhan et al.'s (2012) wave equation. The above analysis suggests that the proposed wave equation can be well used for wavefield simulation and migration imaging. To efficiently solve our newly derived wave equation, we introduce the finite-difference method developed

by Xu and Zhou (2014) as numerical solver. The accuracy of the wavefield simulated by the FD method has been confirmed by the numerical examples. However, as indicated by Liang et al. (2023), the wavefield simulated by the FD method cannot remain the amplitude of anisotropic wavefield. This issue is caused by the construction of the operator S_n. Therefore, to improve wavefield accuracy, one of methods is to develop an optimized operator S_n, which is our future work.

Secondly, the 3D application has received a lot of attention over the years. It is well known that the computational efficiency is dominated problem of the 3D application. The 2D version of the proposed wave equation can be simulated by efficient FD method. This advantage can significantly reduce the computational cost, which can be efficiently used to achieve wavefield simulation and migration imaging in 3D case. In our future work, we will achieve the RTM and LSRTM utilized the proposed wave equation to obtain high-quality imaging results in 3D case.

CONCLUSION

In this paper, we derive a finite-difference solvable pure acoustic wave equation in tilted transversely isotropic media. Compared to coupled pseudo-acoustic equations, the wavefield obtained using the pure acoustic equation remains noise-free and stable when anisotropic parameters $\varepsilon < \delta$. The proposed pure acoustic TTI wave can accurately characterize the qP-wave kinematic behavior. In addition, the newly proposed pure acoustic wave equation demonstrates computational efficiency superior to previous pure acoustic wave equation wave equations solved through spectral-based methods, as illustrated by the computational efficiency analysis. Subsequently, we extend the proposed FD-solvable pure-acoustic TTI wave equation into implement reverse time migration (RTM) in TTI media. Two synthetic examples demonstrate that the imaging results produced by the proposed TTI RTM effectively correct for anisotropic effects, yielding high-quality imaging results. Moreover, due to the high computational efficiency of the proposed wave equation, the proposed TTI RTM technique is conductive for the practical applications for anisotropic media.

ACKNOWLEDEGMENT

REFERENCES

Alkhalifah, T. (1998). Acoustic approximations for processing in transversely isotropic media. *Geophysics* 63 (2), 623-631. doi:10.1190/1.1444361

Alkhalifah, T. (2000). An acoustic wave equation for anisotropic media. *Geophysics* 65 (4), 1239–1250. doi:10.1190/1.1444815

Cheng, J., and Fomel, S. (2014). Fast algorithms for elastic-wave-mode separation and vector decomposition using low-rank approximation for anisotropic media. *Geophysics* 79 (4), C97-C110. doi:10.1190/geo2014-0032.1

Cheng, J., Alkhalifah, T., Wu, Z., Zou, P., and Wang, C. (2016). Simulating propagation of decoupled elastic waves using low-rank approximate mixed-domain integral operators for anisotropic media. *Geophysics* 81 (2), T63-T77. doi:10.1190/geo2015-0184.1

Chu, C., Macy, B. K., and Anno, P. D. (2011). Approximation of pure acoustic seismic wave propagation in TTI media. *Geophysics* 76 (5), WB97-WB107. doi:10.1190/geo2011-0092.1

Chu, C., Macy, B. K., and Anno, P. D. (2013). Pure acoustic wave propagation in transversely isotropic media by the pseudo-spectral method. *Geophys. Prospect.* 61 (3), 556-567. doi:10.1111/j.1365-2478.2012.01077.x

Duveneck, E., Milcik, P., Bakker, P. M. and Perkins, C. (2008). "Acoustic VTI wave equations and their application for anisotropic reverse-time migration," in SEG Technical Program Expanded Abstracts, Las Vegas, Nevada, November 12, 2008, 2186-2190. doi:10.1190/1.3059320

Fletcher, R. P., Du, X., and Fowler, P. J. (2009). Reverse time migration in tilted transversely isotropic (TTI) media. *Geophysics* 74 (6), WCA179-WCA187.doi:10.1190/1.3269902

Fomel, S., Ying, L., and Song, X. (2013). Seismic wave extrapolation using lowrank symbol approximation. *Geophys. Prospect.* 61(3), 526-536. doi: 10.1111/j.1365-2478.2012.01064.x

Grechka, V., Zhang, L., and Rector III, J. W. (2004). Shear waves in acoustic anisotropic media. *Geophysics* 69 (2), 576-582. doi:10.1190/1.1707077

Huang, J., Mao, Q., Mu, X., Yang, J., Ivan, M. S., Liu, Z., and Zhang, S. (2023). Least-squares reverse time migration based on an efficient pure qP-wave equation. *Geophys. Prospect.* doi: 10.1111/1365-2478.13326

Li, B., and Stovas, A. (2021). Decoupled approximation and separate extrapolation of P-and SV-waves in transversely isotropic media. *Geophysics* 86 (4), C133-C142. doi:10.1190/geo2020-0232.1

Li, X., and Zhu, H. (2018). A finite-difference approach for solving pure quasi-P-wave equations in transversely isotropic and orthorhombic media. *Geophysics* 83 (4), C161-C172. doi:10.1190/geo2017-0405.1

Liang, K., Cao, D., Sun, S., and Yin, X. (2023). Decoupled wave equation and forward modeling of qP wave in VTI media with the new acoustic approximation. *Geophysics* 88 (1), WA335-WA344. doi:10.1190/geo2022-0292.1

Mao, Q., Huang, J. P., Mu, X. R., Yang, J. D., and Zhang, Y. J. (2023). Accurate simulations of pure-viscoacoustic wave propagation in tilted transversely isotropic media. *Pet. Sci.* doi: 10.1016/j.petsci.2023.11.005

Mu, X., Huang, J., Yong, P., Huang, J., Guo, X., Liu, D., and Hu, Z. (2020). Modeling of pure qP-and qSV-waves in tilted transversely isotropic media with the optimal quadratic approximation. *Geophysics* 85 (2), C71-C89. doi:10.1190/geo2018-0460.1

Mu, X., Huang, J., Yang, J., Guo, X., and Guo, Y. (2020). Least-squares reverse time migration in TTI media using a pure qP-wave equation. *Geophysics* 85 (4), S199-S216. doi:10.1190/geo2019-0320.1

Nikonenko, Y., and Charara, M. (2021). Efficient acoustic scalar wave equation modeling in VTI media. *Geophysics* 86 (1), T75-T90. doi:10.1190/geo2019-0846.1

Nikonenko, Y., and Charara, M. (2023). Explicit finite-difference modeling for the acoustic scalar wave equation in tilted transverse isotropic media with optimal operators. *Geophysics* 88 (2), T65-T73. doi:10.1190/geo2021-0510.1

Schleicher, J., and Costa, J. C. (2016). A separable strong-anisotropy approximation for pure qP-wave propagation in transversely isotropic media. *Geophysics* 81 (6), C337-C354. doi:10.1190/geo2016-0138.1

Song, X., Fomel, S., and Ying, L. (2013). Lowrank finite-differences and lowrank Fourier finite-differences for seismic wave extrapolation in the acoustic approximation. *Geophys. J. Int.* 193 (2), 960-969. doi:10.1093/gji/ggt017

Stovas, A., Alkhalifah, T., and bin Waheed, U. (2020). Pure P-and S-wave equations in transversely isotropic media. *Geophys. Prospect.* 68 (9), 2762-2769. doi:10.1111/1365-2478.13026

Sun, J., Fomel, S., and Ying, L. (2016). Low-rank one-step wave extrapolation for reverse time migration. *Geophysics* 81 (1), S39-S54. doi:10.1190/geo2015-0183.1

Thomsen, L. (1986). Weak elastic anisotropy. *Geophysics* 51 (10), 1954-1966. doi: 10.1190/1.1442051

Tsvankin, I. (1996). P-wave signatures and notation for transversely isotropic media: An overview. *Geophysics* 61 (2), 467-483. doi:10.1190/1.1443974

Wu, Z., and Alkhalifah, T. (2014). The optimized expansion based low-rank method for wavefield extrapolation. *Geophysics* 79 (2), T51-T60. doi:10.1190/geo2013-0174.1

Xu, S., and Zhou, H. (2014). Accurate simulations of pure quasi-P-waves in complex anisotropic media. *Geophysics* 79 (6), T341-T348. doi:10.1190/geo2014-0242.1

Xu, S., Stovas, A., Alkhalifah, T., and Mikada, H. (2020). New acoustic approximation for transversely isotropic media with a vertical symmetry axis. *Geophysics* 85 (1), C1-C12. doi: 10.1190/geo2019-0100.1

Wang, W., Hua, B., McMechan, G. A., and Duquet, B. (2018). P-and S-decomposition in anisotropic media with localized low-rank approximations. *Geophysics* 83 (1), C13-C26. doi:10.1190/geo2017-0138.1

Yang, J., Zhu, H., McMechan, G., and Yue, Y. (2018). Time-domain least-squares migration using the Gaussian beam summation method. *Geophys. J. Int.* 214 (1), 548-572. doi:10.1093/gji/ggy142

Zhan, G., Pestana, R. C., and Stoffa, P. L. (2012) Decoupled equations for reverse time migration in tilted transversely isotropic media. *Geophysics*, 77(2), 37–45. doi:10.1190/geo2011-0175.1

Zhan, G., Pestana, R. C., and Stoffa, P. L. (2013). An efficient hybrid pseudospectral/finite-difference scheme for solving the TTI pure P-wave equation. *J. Geophys. Eng.* 10 (2), 025004. doi:10.1088/1742-2132/10/2/025004

Zhang, Z. D., Alkhalifah, T., and Wu, Z. (2019). A hybrid finite-difference/low-rank solution to anisotropy acoustic wave equations. *Geophysics* 84 (2), T83-T91. doi:10.1190/geo2018-0333.1

Zhang, Y., Zhang, H., and Zhang, G. (2011) A stable TTI reverse time migration and its implementation. *Geophysics*, 76(3), 3–11. doi:10.1190/1.3554411

Zhou, H., G. Zhang, and R. Bloor. (2006a). "An anisotropic acoustic wave equation for VTI media." in 68th Annual International Conference and Exhibition, EAGE, Extended Abstracts, Vienna, June 12, 2006, H033. doi: 10.3997/2214-4609.201402310.

Zhou, H., G. Zhang, and R. Bloor. (2006b). "An anisotropic acoustic wave equation for modeling and migration in 2D TTI media." in SEG Technical Program Expanded Abstracts, New Orleans, Louisiana, October 3, 2006, 194–198. doi: 10.1190/1.2369913.

Zhu, F., Huang, J., and Yu, H. (2018). Least-squares Fourier finite-difference pre-stack depth migration for VTI media., *J. Geophys. Eng.* 15 (2), 421-437. doi:10.1088/1742-2140/aa9a0a

Zhu, H. (2017). Elastic wavefield separation based on the Helmholtz decomposition. *Geophysics* 82 (2), S173-S183. doi:10.1190/geo2016-0419.1

APPENDIX A

Stability condition for the proposed 2D TTI pure qP-wave equation

Equation (16) can be rewritten as

$$
p_{i,j}^{n+1} = -v_p^2 \Delta t^2 \left\{ \begin{aligned} & \left((1+2\varepsilon)\cos^2\theta + \sin^2\theta \right)k_x^2 + \left((1+2\varepsilon)\sin^2\theta + \cos^2\theta \right)k_z^2 - 2\varepsilon\sin 2\theta k_x k_z - 2(\varepsilon - \delta)/(1-0.5\varepsilon) \times \\ & \left((1-0.5\delta - 2\varepsilon)\cos^4\theta\sin^2\theta + (1-0.5\delta)\cos^2\theta\sin^4\theta \right)\frac{k_x^6}{\left(k_x^2+k_z^2\right)^2} + \\ & \left((1-0.5\delta - 2\varepsilon)\left(\cos^4\theta\sin 2\theta - 0.5\sin^3 2\theta\right) + (1-0.5\delta)\left(0.5\sin^3 2\theta - \sin^4\theta\sin 2\theta\right) \right)\frac{k_x^5 k_z}{\left(k_x^2+k_z^2\right)^2} + \\ & \left((1-0.5\delta - 2\varepsilon)\left(\cos^6\theta + 1.5\sin^2\theta\sin^2 2\theta - 2\cos^2\theta\sin^2 2\theta\right) + (1-0.5\delta)\left(\sin^6\theta + 1.5\cos^2\theta\sin^2 2\theta - 2\sin^2\theta\sin^2 2\theta\right) \right)\frac{k_x^4 k_z^2}{\left(k_x^2+k_z^2\right)^2} + \\ & \left((1-0.5\delta - 2\varepsilon)\left(1.5\sin^3 2\theta - 2\cos^4\theta\sin 2\theta - 2\sin^4\theta\sin 2\theta\right) + (1-0.5\delta)\left(-1.5\sin^3 2\theta + 2\cos^4\theta\sin 2\theta + 2\sin^4\theta\sin 2\theta\right) \right)\frac{k_x^3 k_z^3}{\left(k_x^2+k_z^2\right)^2} + \\ & \left((1-0.5\delta - 2\varepsilon)\left(\sin^6\theta - 2\sin^2\theta\sin^2 2\theta + 1.5\cos^2\theta\sin^2 2\theta\right) + (1-0.5\delta)\left(\cos^6\theta - 2\cos^2\theta\sin^2 2\theta + 1.5\sin^2\theta\sin^2 2\theta\right) \right)\frac{k_x^2 k_z^4}{\left(k_x^2+k_z^2\right)^2} + \\ & \left((1-0.5\delta - 2\varepsilon)\left(-0.5\sin^3 2\theta + \sin^4\theta\sin 2\theta\right) + (1-0.5\delta)\left(0.5\sin^3 2\theta - \cos^4\theta\sin 2\theta\right) \right)\frac{k_x^5 k_x}{\left(k_x^2+k_z^2\right)^2} + \\ & \left((1-0.5\delta - 2\varepsilon)\sin^4\theta\cos^2\theta + (1-0.5\delta)\cos^4\theta\sin^2\theta \right)\frac{k_z^6}{\left(k_x^2+k_z^2\right)^2} \end{aligned} \right\} p_{i,j}^n + 2p_{i,j}^n - p_{i,j}^{n-1},\; \text{(A-1)}
$$

where i and j denote the spatial grid indices for the *x*- and *z*-axes, respectively. p is the pressure wavefield, n is time index. The matrix form of equation (A-1) is

$$
\begin{bmatrix} p_{i,j}^{n+1} \\ p_{i,j}^n \end{bmatrix} = \begin{bmatrix} A\Delta t^2 + 2 & -1 \\ 1 & 0 \end{bmatrix} \begin{bmatrix} p_{i,j}^n \\ p_{i,j}^{n-1} \end{bmatrix} \tag{A-2}
$$

and

$$
A = -v_p^2 \left\{ \begin{aligned} & \left((1+2\varepsilon)\cos^2\theta + \sin^2\theta \right)k_x^2 + \left((1+2\varepsilon)\sin^2\theta + \cos^2\theta \right)k_z^2 - 2\varepsilon\sin 2\theta k_x k_z - 2(\varepsilon - \delta)/(1-0.5\varepsilon) \times \\ & \left((1-0.5\delta - 2\varepsilon)\cos^4\theta\sin^2\theta + (1-0.5\delta)\cos^2\theta\sin^4\theta \right)\frac{k_x^6}{\left(k_x^2+k_z^2\right)^2} + \\ & \left((1-0.5\delta - 2\varepsilon)\left(\cos^4\theta\sin 2\theta - 0.5\sin^3 2\theta\right) + (1-0.5\delta)\left(0.5\sin^3 2\theta - \sin^4\theta\sin 2\theta\right) \right)\frac{k_x^5 k_z}{\left(k_x^2+k_z^2\right)^2} + \\ & \left((1-0.5\delta - 2\varepsilon)\left(\cos^6\theta + 1.5\sin^2\theta\sin^2 2\theta - 2\cos^2\theta\sin^2 2\theta\right) + (1-0.5\delta)\left(\sin^6\theta + 1.5\cos^2\theta\sin^2 2\theta - 2\sin^2\theta\sin^2 2\theta\right) \right)\frac{k_x^4 k_z^2}{\left(k_x^2+k_z^2\right)^2} + \\ & \left((1-0.5\delta - 2\varepsilon)\left(1.5\sin^3 2\theta - 2\cos^4\theta\sin 2\theta - 2\sin^4\theta\sin 2\theta\right) + (1-0.5\delta)\left(-1.5\sin^3 2\theta + 2\cos^4\theta\sin 2\theta + 2\sin^4\theta\sin 2\theta\right) \right)\frac{k_x^3 k_z^3}{\left(k_x^2+k_z^2\right)^2} + \\ & \left((1-0.5\delta - 2\varepsilon)\left(\sin^6\theta - 2\sin^2\theta\sin^2 2\theta + 1.5\cos^2\theta\sin^2 2\theta\right) + (1-0.5\delta)\left(\cos^6\theta - 2\cos^2\theta\sin^2 2\theta + 1.5\sin^2\theta\sin^2 2\theta\right) \right)\frac{k_x^2 k_z^4}{\left(k_x^2+k_z^2\right)^2} + \\ & \left((1-0.5\delta - 2\varepsilon)\left(-0.5\sin^3 2\theta + \sin^4\theta\sin 2\theta\right) + (1-0.5\delta)\left(0.5\sin^3 2\theta - \cos^4\theta\sin 2\theta\right) \right)\frac{k_x^5 k_x}{\left(k_x^2+k_z^2\right)^2} + \\ & \left((1-0.5\delta - 2\varepsilon)\sin^4\theta\cos^2\theta + (1-0.5\delta)\cos^4\theta\sin^2\theta \right)\frac{k_z^6}{\left(k_x^2+k_z^2\right)^2} \end{aligned} \right\} \cdot \text{(A-3)}
$$

To ensure the numerical simulation stability of equation (A-1), the time step sampling should meet the definition as follow (Yang and Zhu, 2018; Mu et al., 2020b):

$$
\Delta t \le \left| \frac{\sqrt{-2A}}{-A} \right| < \sqrt{\frac{-2}{A_{\min}}}, \tag{A-4}
$$

where Δt is time sampling step, $A_{\min}$ is the minimum value of A. In most cases, ε is larger than δ. Therefore, $A_{\min}$ can be expressed as

$$A_{\min} = -v_p^2 \left(\left((1+2\varepsilon)\cos^2\theta + \sin^2\theta \right) k_x^2 + \left((1+2\varepsilon)\sin^2\theta + \cos^2\theta \right) k_z^2 - 2\varepsilon\sin 2\theta k_x k_z \right). \tag{A-5}$$

Assuming that $\Delta x = \Delta z = \Delta d$ and the Nyquist wavenumber $k_{Nyq} = \pi / \Delta d$, we can obtain

$$0 \le k_x k_z \le k_{Nyq}^2, \tag{A-6}$$

and

$$A_{\min} = -v_p^2 \left(\left((1+2\varepsilon)\cos^2\theta + \sin^2\theta \right) k_{Nyq}^2 + \left((1+2\varepsilon)\sin^2\theta + \cos^2\theta \right) k_{Nyq}^2 - \left(2\varepsilon\sin 2\theta \right) k_{Nyq}^2 \right). \tag{A-7}$$

Finally, the time sampling in TTI media can be expressed as

$$\Delta t < \frac{\Delta d}{\pi v_{p\max} \sqrt{1 + \varepsilon_{\max} + \varepsilon_{\max} \left(\sin 2\theta \right)_{\max}}}. \tag{A-8}$$